

A dual-mode quantum dot laser operating in the excited state

F. Grillot, N. A. Naderi, J. B. Wright, R. Raghunathan, M. T. Crowley et al.

Citation: *Appl. Phys. Lett.* **99**, 231110 (2011); doi: 10.1063/1.3667193

View online: <http://dx.doi.org/10.1063/1.3667193>

View Table of Contents: <http://apl.aip.org/resource/1/APPLAB/v99/i23>

Published by the [American Institute of Physics](#).

Additional information on *Appl. Phys. Lett.*

Journal Homepage: <http://apl.aip.org/>

Journal Information: http://apl.aip.org/about/about_the_journal

Top downloads: http://apl.aip.org/features/most_downloaded

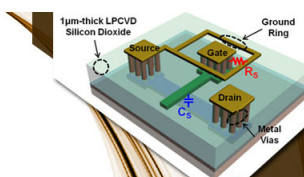
Information for Authors: <http://apl.aip.org/authors>

ADVERTISEMENT



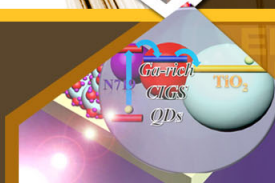
**EXPLORE WHAT'S
NEW IN APL**

SUBMIT YOUR PAPER NOW!



SURFACES AND INTERFACES

Focusing on physical, chemical, biological, structural, optical, magnetic and electrical properties of surfaces and interfaces, and more...



ENERGY CONVERSION AND STORAGE

Focusing on all aspects of static and dynamic energy conversion, energy storage, photovoltaics, solar fuels, batteries, capacitors, thermoelectrics, and more...

A dual-mode quantum dot laser operating in the excited state

F. Grillot,^{1,2,a)} N. A. Naderi,³ J. B. Wright,⁴ R. Raghunathan,³ M. T. Crowley,³
and L. F. Lester³

¹Université Européenne de Bretagne, INSA, CNRS, Laboratoire FOTON, 20 Avenue des buttes de Coesmes, 35708 Rennes Cedex 7, France

²Institut TELECOM/Telecom Paristech, CNRS LTCI, 75634 Paris Cedex, France

³Center for High Technology Materials, University of New Mexico, 1313 Goddard SE, Albuquerque, New Mexico 87106, USA

⁴Sandia National Laboratories, 1515 Eubank SE, Albuquerque, New Mexico 87185, USA

(Received 25 October 2011; accepted 16 November 2011; published online 9 December 2011)

A dual-mode laser operating in the excited states (ESs) of a quantum dot is realized by combining asymmetric pumping and external optical feedback stabilization. In generating two single-mode emission peaks, a mode separation ranging from 1.3-THz to 3.6-THz is demonstrated over temperature. This effect is attributed to the unique carrier dynamics of the quantum-dot gain medium via the excited state inhomogeneous linewidth coupled with a proper external control. These results are particularly important towards the development of future THz optoelectronic sources with compact size, low fabrication cost, and high performance. © 2011 American Institute of Physics. [doi:10.1063/1.3667193]

Applications pertaining to THz radiation are both diverse and many, encompassing homeland security, computing and communications technologies, medical and pharmaceutical fields, as well as basic material science.¹⁻⁶ THz waves can be generated by coherently interfering two optical modes, which are generated by two separate single-mode lasers. The light is then absorbed in an ultrafast photoconductive semiconductor.⁷⁻⁹ An alternative approach simultaneously generates dual wavelength emission from a single laser cavity. This approach has the advantage of being free of optical alignment issues since there is no need to align two laser beams—a critical requirement for photomixing efficiency. Typically, dual wavelength emission from quantum well (QW) lasers requires two separate gratings to be incorporated into the device. Furthermore, the tunability associated with these devices is limited by the bandwidth of the QW gain profile.¹⁰ By contrast, quantum dot (QD) lasers offer a more flexible platform to generate tunable dual-wavelength emission. Simultaneous ground state (GS) and excited state (ES) operation with multi-mode emission has been previously observed in QD lasers and was attributed to the incomplete clamping of the ES carrier population at the GS threshold, in contrast to the complete clamping of the threshold carrier density associated with QW lasers.¹¹ Due to the relatively low density of states inherent to QDs and consequent unique carrier dynamics, dual-wavelength emission consisting of a single distributed feedback (DFB) mode and a single Fabry-Perot (FP) mode, both originating from the same inhomogeneously broadened QD transition can be realized. This phenomenon of accessing different carrier populations in an inhomogeneously broadened system is not likely in a QW active region because of the contrasting carrier dynamics associated with a homogeneously broadened continuous density of states.¹² The wide gain bandwidth

characteristic of QD nanostructures enables a relatively large frequency difference between the two modes.

Recently, dual-mode emission was demonstrated in a two-section QD laser where one mode was coupled to a Bragg grating and the other to the FP cavity.¹³ It was shown that the relative spectral intensities between the QD GS and ES modes could be equalized, resulting in a simultaneous dual-mode emission with an 8-THz frequency difference. Following the same concept with a similar device, this paper focuses on the generation of dual-modes from the QD ES only with one peak being coupled to the grating and the other to the FP cavity. By appropriately combining asymmetric pumping with controlled optical feedback, it is shown that the observed mode frequency difference can be tuned from 1.3-THz to 3.6-THz over a wide temperature range. These results are enabled through the unique nature of the QD media via the ES inhomogeneous linewidth and are also coupled with the effects of using an external stabilization mechanism. The technical approach described in this paper addresses the need for compact size and low fabrication cost, which is significant for the development of future THz optoelectronic sources.

Device fabrication and epitaxial structure details of the two-section dual mode QD laser can be found elsewhere.¹³ Figure 1 shows the light current characteristics $L(I)$ measured under uniform pumping and at different temperatures from 5 °C to 40 °C. The device was mounted on a heat sink using conductive epoxy and the temperature is thermoelectrically controlled. From Fig. 1, one can see that the device turns on at the QD ES for threshold currents ranging from 55-mA at 5 °C up to 120-mA at 40 °C. The inset in Fig. 1 shows the optical spectrum of the solitary laser recorded at 20 °C and under an asymmetrical bias condition where the total pump current was 130-mA (75 mA/55 mA). The result shows that the ES lasing takes place at 1192.4 nm with a side mode suppression ratio (SMSR) greater than 40-dB. This strong single emission demonstrates that the lasing peak is

^{a)} Author to whom correspondence should be addressed. Electronic mail: frederic.grillot@insa-rennes.fr.

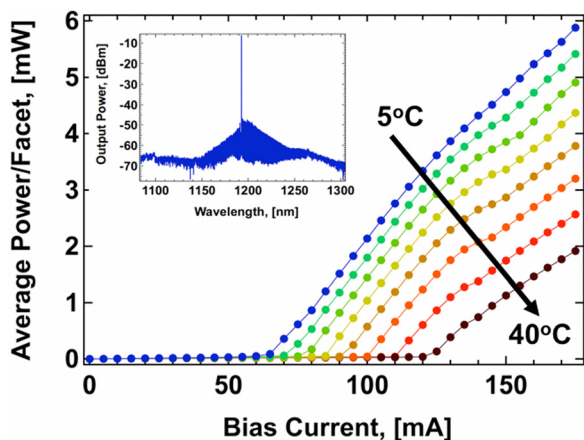


FIG. 1. (Color online) The L(I) characteristics of the QD dual-mode laser at different temperatures from 5 °C to 40 °C. The inset shows the optical spectrum of the solitary laser under asymmetric pumping and at room temperature.

coupled to the DFB mode of the device. Similar single-mode operation can be obtained under symmetric current injection.¹² Figure 2 presents the observed cavity mode shifts of the DFB and FP peaks at different temperatures, ranging from 5 °C to 40 °C, for both uniform and asymmetrical optical pumping conditions. Solid symbols correspond to the actual measurements while the solid lines represent the curve-fittings. The results in Fig. 2 show that regardless of the pumping conditions, the cavity mode shift of the DFB peak remains roughly constant at about 0.10 nm/°C while that of the FP modes is larger at 0.16 nm/°C.

In order to increase the laser's stability as well as to manipulate the different FP cavity modes, an optical fiber-based feedback loop is implemented in the experimental setup. The feedback loop to the laser consisted of a four-port polarization-maintaining (PM) 50/50 fiber coupler. The DFB laser output light was injected into port 1, and the optical feedback was then created using a high-reflectivity coated fiber connected to port 2. The applied external feedback level was controlled via a fiber-based variable attenuator at port 4. The impact of the external optical feedback on the laser spectrum was analyzed with a resolution of 10 pm. The distance between the laser and the external reflector is estimated to be a few meters, which corresponds to an external round-trip time of about 10–30 ns (long external cavity condition).¹⁴ The amount of injected optical feedback into the

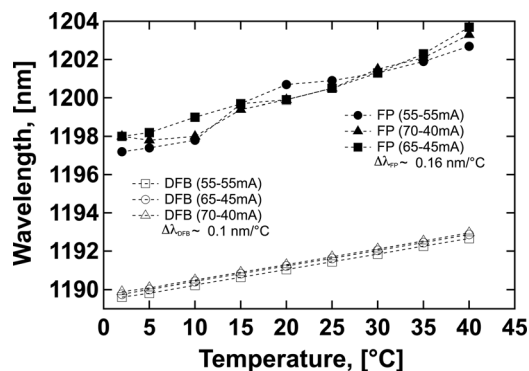


FIG. 2. DFB and Fabry-Perot cavity mode shifts as a function of temperature for different pumping conditions.

laser, Γ , is defined as the ratio between the reflected power and the emitted power. Figure 3(a) shows the optical spectra recorded under asymmetric pumping at the lowest temperature (5 °C) and for a total pump current of 115-mA (66.5-mA/48.5-mA). In Fig. 3(a), the red spectrum corresponds to the solitary laser while the blue one is obtained for an optimum feedback level of $\Gamma = 2 \times 10^{-3}$. Results show that optimizing the applied external feedback conditions leads to the generation of an additional mode lasing at 1208.1-nm and related to the FP cavity, which is also located within the ES inhomogeneously broadened bandwidth. Since the ES DFB peak remains robust and stable as a result of strong Bragg gratings, a dual-mode emission with 3.6-THz frequency difference is demonstrated. Figure 3(b) shows similar results for the highest temperature (40 °C) but for a total pump current of 153-mA (86-mA/67-mA). Although the total pump current had to be increased to compensate for temperature-related effects, it is important to note that the ratio of current in each section was kept constant at around 1.3 throughout the entire experiment. Under the highest achievable optical feedback level of $\Gamma = 4 \times 10^{-3}$, a separate FP-generated peak excites at 1200.1 nm, which is 8-nm away from the grating coupled ES mode. This configuration leads to dual-mode emission with a 1.3-THz frequency difference. In order to summarize the experimental findings, the variations of the frequency difference (left axis) over temperature as well as the corresponding SMSR (right axis) are illustrated in Fig. 4. In this figure, each point is measured for the configuration that yielded the optimum optical feedback condition. Solid lines in Fig. 4 are used as a guide for the eye.

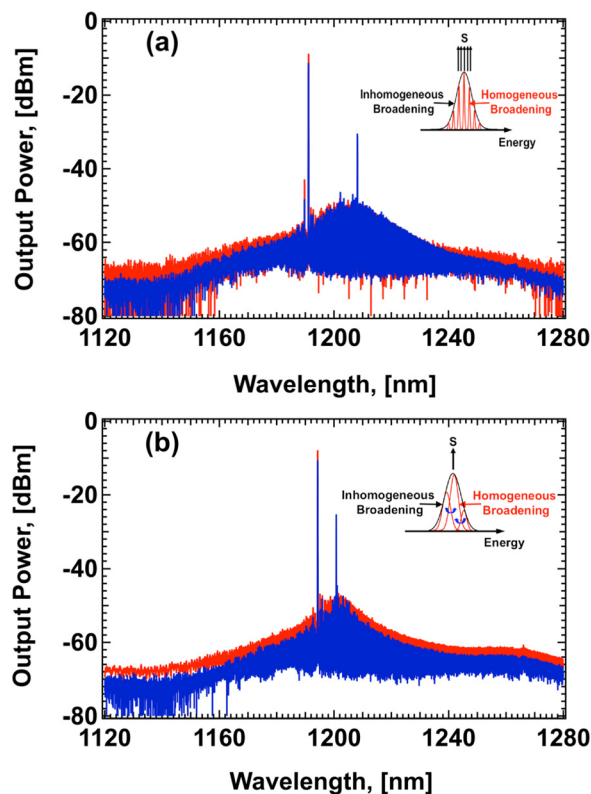


FIG. 3. (Color online) Spectra under total asymmetric pump current for the solitary laser (strong peak at shorter wavelength) and under controlled optical feedback (two strong peaks) at (a) 5 °C and (b) 40 °C.

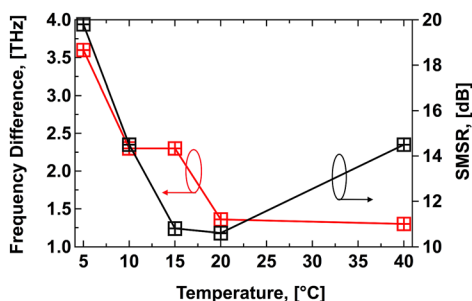


FIG. 4. (Color online) Measured THz frequency difference (data decreasing with temperature) and side mode suppression ratio, data showing a minimum at 15-20 °C, as a function of temperature under the best optical feedback conditions. Solid lines are a guide for the eyes.

Based on these results, it can be deduced that the frequency difference is progressively tuned closer to the gain peak from 3.6-THz all the way down to 1.3-THz when the temperature is decreased successively from 40 °C to 5 °C. The corresponding SMSR ranged from 10-dB to 20-dB meaning that in all cases studied here, the two peak powers could not be equalized due to the limited optical feedback amplitude as well as the loss induced by the fiber-based feedback setup. The optical feedback is known to induce variations in stimulated emission, which are provoked by the beating of the photons with the delayed field. Consequently, the carrier fluctuations related to the cavity photons can deplete carriers from both resonant QD states inside the homogenous broadening as well as non-resonant states outside. The small decrease in the DFB peak power under optical feedback can be explained by the carrier depletion of the resonant QD states, which are transferred to another dot population. As shown in Fig. 2, the DFB and FP cavity mode shifts do not exceed 0.10-nm/°C and 0.16-nm/°C, respectively, therefore, these variations alone cannot explain the change in the observed frequency difference with temperature. Another important point to take into account is the temperature and injected current level dependence of the homogenous broadening.¹¹ At low temperature, dots with different energies remain spatially isolated from each other (see inset of Fig. 3(a)) while they get spatially and energetically connected to each other at higher temperatures (inset of Fig. 3(b)). Finally, the homogeneous linewidth also increases with increasing current injection.¹⁵ These three effects can cause the homogeneous broadening to vary from 5-meV to 30-meV and can, although other effects may be present, explain the progressive shift with temperature of the resonant mode towards the ES gain peak. Although simultaneous GS and ES with multi-mode emissions have been previously observed in QD mate-

rial when increasing the bias current well above threshold,^{12,16} the results presented here demonstrate dual-mode operation exclusively from the QD ES. To conclude, dual-mode lasing within the ES inhomogeneous broadening can be manipulated via a suitable combination of asymmetric pumping and external optical feedback in a two-section QD laser. This technique could enable THz frequency generation ranging from 1.3-THz to 3.6-THz. Compared to existing technologies, the technical approach described in this paper has potential for implementation in a compact and low-cost THz source.

This work was performed, in part, at the Center for Integrated Nanotechnologies, a U.S. Department of Energy, Office of Basic Energy Sciences user facility at Los Alamos National Laboratory (Contract No. DE-AC52-06NA25396) and Sandia National Laboratories (Contract No. DE-AC04-94AL85000). This work was supported by the Air Force Office of Scientific Research under Grant No. FA9550-10-1-0276.

¹M. Koch, *Terahertz Frequency Detection and Identification of Materials and Objects*, edited by R. E. Miles, X. C. Zhang, H. Eisele, and A. Krotkus (Springer, New York, 2007).

²P. H. Siegel, *IEEE Trans. Microwave Theory Tech.* **52**, 2438 (2004).

³P. F. Taday, *Philos. Trans. R. Soc. London* **362**, 351 (2004).

⁴S. Wang, B. Ferguson, D. Abbott, and X.-C. Zhang, *J. Biol. Phys.* **29**, 247 (2003).

⁵M. Naftaly and R. E. Miles, *Terahertz time-domain spectroscopy for material characterization*, Proceedings of the IEEE, vol. 95 (2007), pp. 1658–1665.

⁶C. Baker, T. Lo, W. R. Tribe, B. E. Cole, M. R. Hogbin, and M. C. Kemp, *Detection of concealed explosives at a distance using terahertz technology*, Proceedings of IEEE on T-Ray Imaging, Sensing, and Retention Proc. IEEE, vol. 95, (2007), pp. 1559–1565.

⁷R. Mendis, C. Sydlo, J. Sigmund, M. Feiginov, P. Meissner, and H. L. Hartnagel, *Int. J. Infrared Millim. Waves* **26**, 201 (2005).

⁸M. Tani, O. Morikawa, S. Matsuura, and M. Hangyo, *Semicond. Sci. Technol.* **20**, S151 (2005).

⁹M. Naftaly, M. R. Stone, A. Malcoci, R. E. Miles, and I. C. Mayorga, *Electron. Lett.* **41**, 128 (2005).

¹⁰S. D. Roh, T. S. Yeoh, R. B. Swint, A. E. Huber, C. Y. Woo, J. S. Hughes, and J. J. Coleman, *IEEE Photon. Technol. Lett.* **12**, 1307 (2000).

¹¹F. Grillot, K. Veselinov, M. Gioannini, I. Montrosset, J. Even, R. Piron, E. Homeyer, and S. Loualiche, *IEEE J. Quantum Electron.* **45**, 872 (2009).

¹²A. Markus, J. X. Chen, C. Paranthoen, and A. Fiore, *Appl. Phys. Lett.* **82**, 1818 (2003).

¹³N. A. Naderi, F. Grillot, A. Gin, and L. F. Lester, *Opt. Express* **18**, 27028 (2011).

¹⁴D. M. Kane and K. A. Shore, *Unlocking Dynamical Diversity* (Wiley, New York, 2005).

¹⁵P. Borri, W. Langbein, S. Schneider, U. Woggon, R. L. Sellin, D. Ouyang, and D. Bimberg, *IEEE J. Sel. Top. Quantum Electron.* **8**, 984 (2002).

¹⁶M. A. Cataluna, D. I. Nikitichev, S. Mikroulis, H. Simos, C. Simos, C. Mesaritis, D. Syvridis, I. Krestnikov, D. Livshits, and E. U. Rafailov, *Opt. Express* **18**, 12832 (2010).